American Mineralogist, Volume 72, pages 1131–1143, 1987

Laser-interference and Nomarski interference imaging of zoning profiles in plagioclase phenocrysts from the May 18, 1980, eruption of Mount St. Helens, Washington

T. H. Pearce
Department of Geological Sciences, Queen's University, Kingston, Ontario K7L 3N6, Canada
J. K. Russell
Department of Geological Sciences, University of British Columbia, Vancouver, British Columbia V6T 2B4, Canada
I. Wolfson
Department of Geological Sciences, Queen's University, Kingston, Ontario K7L 3N6, Canada

Abstract

Laser-interference microscopy, Nomarski interference-contrast microscopy (on etched polished sections), petrographic microscopy, and electron-microprobe analysis have been used to study the phenocryst population of a sample of pumice from the May 18, 1980, eruption of Mount St. Helens. The pumice appears to contain more than one population of phenocrysts and may itself be a sample of different layers in a zoned magma chamber. An overlapping sequence of events can be determined for the two most common phenocryst types. A model developed from the zoning profiles involves an early stage of growth at depth followed by a period of massive resorption of all phenocryst phases. The apparent resorption of hornblende with no sign of magmatic reaction or opacite rims is remarkable. Plagioclase compositions range from An_{63} to An_{37}, with the commonest composition being An_{46}. There appears to be a general similarity between the zoning pattern in the mantles of the larger phenocrysts (type I) and the complete zoning pattern of the smaller euhedral phenocrysts (type II). We consider that this is due to contemporaneous growth. In spite of overall similarities in zoning profiles, there are inconsistencies in both the compositions and the number and type of resorption events. Exact correlation between specific events cannot be drawn pending more detailed magmatic stratigraphic correlation between phenocrysts.

Introduction

The May 18, 1980, eruption of Mount St. Helens produced a gray pumice containing small crystals of plagioclase, orthopyroxene, hornblende, and opaques set in a highly vesicular glass matrix (Kuntz et al., 1981). The known and postulated pre-eruption history of this rock is well constrained by experimental work (see outline below). We expected, therefore, that the observed population of crystals in the pumice would be fairly simple. However, we have observed complexities in the phenocryst population that were not entirely expected, and in this work we report our preliminary observations. We will emphasize petrographic interpretations based mainly on zoning patterns observed by interference imaging.

The Quaternary geologic setting of the Mount St. Helens area has been outlined by Leeman and Smith (1982). The lateral blast and pyroclastic products of the May 18, 1980, eruption have been studied in detail by many researchers, and interested readers are referred in particular to the U.S. Geological Survey Professional Paper on Mount St. Helens (Lipman and Mullineaux, 1981). An extraordinary amount of information on the products of this eruption is available, and we expect our present results, obtained by using some novel observational techniques, will complement the exisiting studies of volcanic products of this most interesting volcano.

The sample that we used in this work is a pumice fragment of the May 18, 1980, pyroclastic flow collected near the northeastern flank of the Mount St. Helens "pumice plain" (Rowley et al., 1981). Plagioclase crystals in both thin and polished thin sections were examined optically by standard petrographic microscopy, laser-interference microscopy, and, after etching, in reflected light by Nomarski interference-contrast microscopy. Absolute plagioclase compositions were determined by electron-microprobe and standard optical methods.

Experimental constraints

The experimental work of Merzbacher and Eggler (1984) and Sigurdsson et al. (1984) restricts the P-T-X_{H_2O} phase relations of the Mount St. Helens magma. Melting experiments of the MSH pumice (Sigurdsson et al., 1984)

0003–004X/87/1112–1131$02.00

TABLE 1. Representative electron-microprobe analyses of feldspars from the Mount St. Helens pumice

	MSH-A-1		MSH-A-3		MSH-A-5		MSH-B-1	
	An	Ab	An	Ab	An	Ab	An	Ab
SiO_2	55.77	58.97	55.36	58.86	51.95	56.23	53.25	59.01
Al_2O_3	28.71	25.36	28.43	25.51	30.12	26.75	30.12	26.16
FeO	0.36	0.32	0.37	0.26	0.39	0.31	0.33	0.34
MgO	b.d.	b.d.	b.d.	b.d.	b.d.	b.d.	b.d.	b.d.
CaO	10.46	7.91	10.67	7.82	13.06	9.70	12.43	7.88
Na_2O	5.62	6.96	5.44	7.13	4.10	5.98	4.48	6.98
K_2O	0.12	0.19	0.12	0.21	0.06	0.14	0.10	0.21
Total	101.04	99.71	100.39	99.79	99.68	99.11	100.71	100.58
X_{An}	50.35	38.16	51.65	37.29	63.55	46.89	60.18	37.96
X_{Ab}	48.96	60.75	47.66	61.52	36.10	52.31	39.25	60.84
X_{Or}	0.69	1.09	0.69	1.19	0.35	0.81	0.58	1.20

Note: Structural formulae are calculated with all Fe treated as Fe^{3+}. Reported analyses represent the extreme compositions that were analyzed expressed as weight percent oxides (calculations after Nicholls and Stout, 1986).

indicate that the observed phase assemblage, with the exception of amphibole, can be reproduced from similar melt compositions that are undersaturated with respect to water. The experimental conditions that best reproduced the observed phase assemblage were 930 ± 10 °C, 220 ± 30 MPa confining pressure, and $P_{H_2O}/P_{total} = 0.5$–0.7. Under these conditions, however, amphibole was not stable. Merzbacher and Eggler (1984) explained crystallization of amphibole in the natural system by higher values of P_{H_2O}, perhaps induced by crystallization.

More recent experimental work by Rutherford and Devine (1986) has established that, in contrast to the earlier work at $\log f_{O_2} = -11.3$ (Ni-NiO buffer), a $\log f_{O_2} = -10.0$ will stabilize amphibole in the natural liquid. These newest results indicate that the natural assemblage is stable at 920 °C, 220 MPa (2.2 kbar) and H_2O contents as low as 4.6% with $P_{H_2O}/P_{fluid} = 0.67$. Glass inclusions in the natural amphibole contain 5.8% volatiles and appear to be slightly less evolved (in terms of Al_2O_3 and SiO_2) than those in the natural plagioclase. The plagioclase in the experimental runs decreased in An content with decreasing P_{H_2O}/P_{fluid}, reaching An_{50} when $P_{H_2O}/P_{fluid} = 0.64$.

From this experimental work, we assume that at some pre-eruptive stage in its history, the May 18, 1980, dacite magma (with 4 to 5% H_2O) was held in a magma chamber at 220 MPa (6- to 7-km depth) where it crystallized at about 920 °C to an assemblage of plagioclase, orthopyroxene, iron oxide, amphibole, minor clinopyroxene, and co-existing melt. When the magma erupted, it contained approximately 35% crystals.

Did the magma move directly to the surface—essentially erupting from 220 to 0 MPa—in one rapid event, a model consistent with that proposed by Rutherford et al. (1985)? Did the magma pause subvolcanically prior to eruption? Do the crystals in the dacite represent crystallization at a single depth or at various levels in a vertically zoned magma chamber (consistent with the results of Melson, 1983)? Is there evidence in the crystal populations of any earlier magmatic phases? We expect that evidence for such complications in the crystallization of a magma might be preserved in the zonal stratigraphy of phenocrysts. We hope that this present work will add detail to existing knowledge of the crystallization history of the May 18, 1980, pumice of Mount St. Helens.

→

Fig. 1. Two examples of finely zoned type II plagioclase showing even-oscillatory and normal-oscillatory zoning. (A) photomicrograph (cross-polarized light) of crystal MSH-D-9. (B) Nomarski image of the etched surface of crystal MSH-D-9. Note the enhanced visibility of very fine zoning in this crystal. There are more than 28 zones with an average thickness of 4.8 μm. The arrows point to discontinuities in the zoning due to resorption. (C) Narrow-fringe laser interferogram of crystal MSH-D-9 taken in green light (514.5-nm wavelength) from an Ar-ion laser. Note the apparently flat core and the flat average composition in the mantle. There are sudden jumps in the An content on the outside of the discontinuities that are interpreted as resorption layers ("R"). These calcic jumps rarely exceed 10 mol% An but may locally be as great as 20 mol% An. (D) Digitized profile of the interferogram in Fig. 1C (traverse X to C) showing An content as a function of distance from the rim in the crystal. Note that some of the finer oscillations cannot be resolved on this scale and have been smoothed out. (E) Plane-polarized-light view of crystal MSH-B-1. Note the concentric arrangement of acicular apatite (A) along the outer zone of the crystal. (F) Nomarski image of the etched surface of crystal MSH-B-1. Note the enhanced visibility of the very fine zoning in this crystal. The section goes almost completely through the center of the crystal, which contains over 30 zones. Note the euhedral nature of most of the zones. "R" indicates a resorption surface. (G) Narrow-fringe laser interferogram (514.5 nm) of crystal MSH-B-1. Note that the pattern is for the most part normally zoned. (H) Digitized profile of the interferogram in Fig. 1G showing An content as a function of distance from the rim along traverse XY. The minor oscillations in composition have been smoothed over in this representation of the zoning.

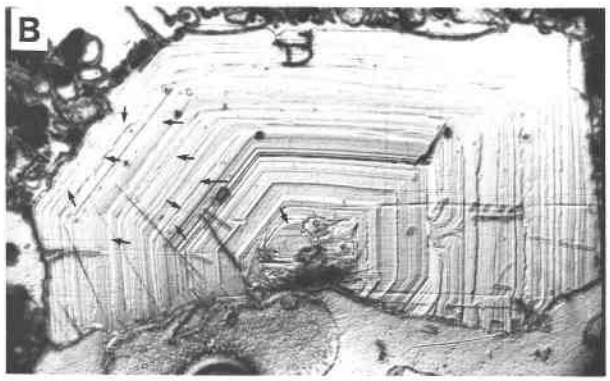

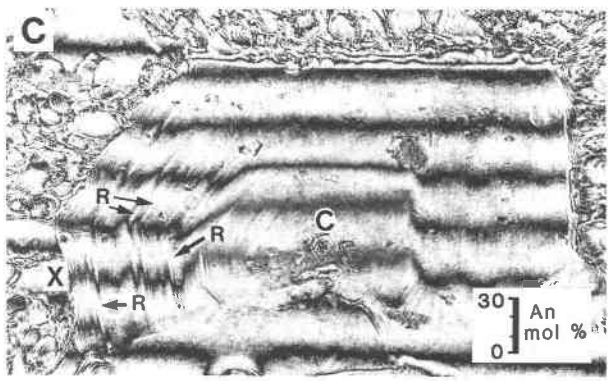

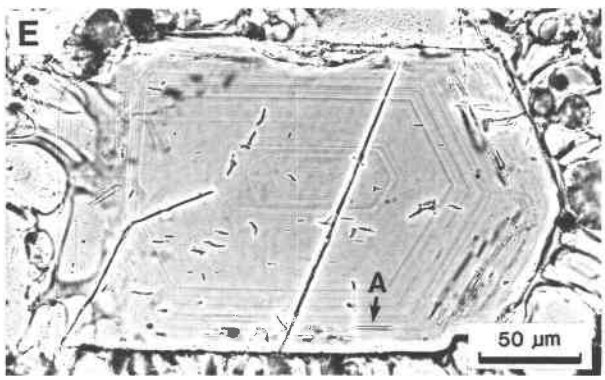

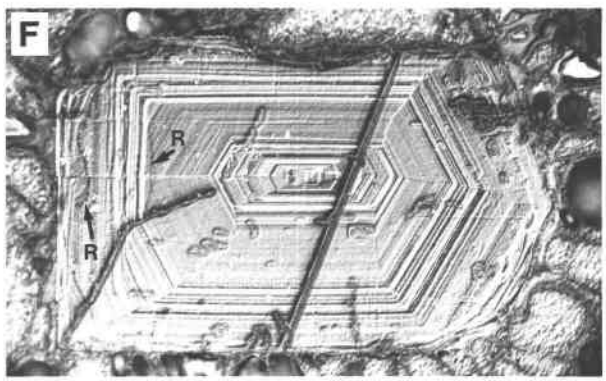

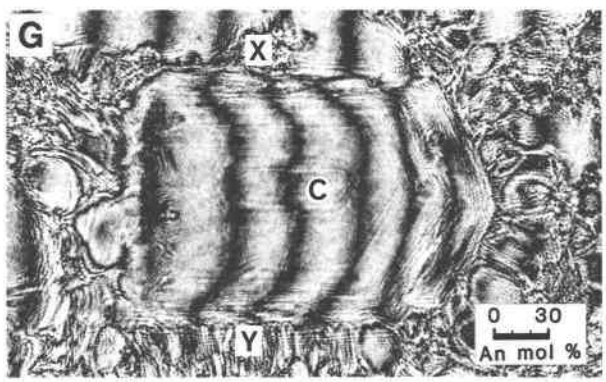

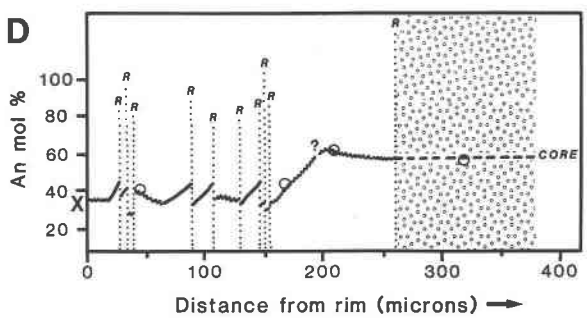

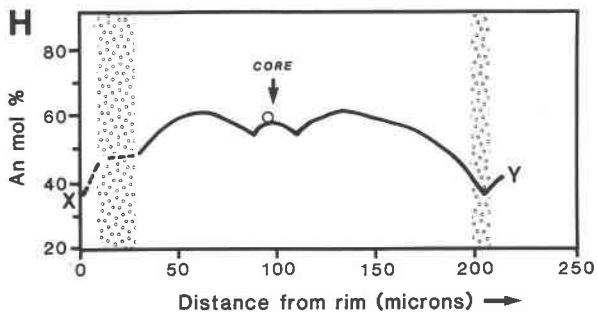

fringe trace

approximate fringe trace

trace of fine, unresolvable oscillatory zoning

?— calcic 'spike', of indeterminate composition

inclusion rich zone

R resorption surface

point of microprobe analysis

Theory and methods of analysis

Four polished thin sections and three thin sections cut from the same pumice block were examined. Each polished thin section contained over 800 plagioclase phenocrysts. About twelve representative crystals per slide were chosen for closer scrutiny by laser and Nomarski techniques. Optimum crystals were those sectioned through or near their core and oriented so that one of the crystal faces was vertical. This ensured that the zonation parallel to that face was perpendicular to the plane of the section (see Pearce, 1984a, for further discussion). Absolute plagioclase compositions were obtained by electron microprobe. Each of these techniques is described in detail below.

Electron microprobe

Feldspar compositions were determined with an ARL-SEMQ electron microprobe at the University of Calgary. Standard operating conditions for feldspar analysis were followed including 15-kV accelerating voltage, 300-μA emission current, and 0.15-μA beam current (Nicholls and Stout, 1986). The beam diameter used during analysis was estimated from the luminescence of MgO to be approximately 2 μm. Spectra for eight elements were collected synchronously on wavelength-dispersive spectrometers. The data were reduced to weight percent oxides with Bence-Albee (1968) correction methods as programmed by Nicholls et al. (1977). The feldspars were analyzed for BaO, MgO, and FeO in addition to the major oxide constituents. BaO was not detected, and MgO concentrations were also below or at detection. FeO was found to range from 0.20 to 0.50 wt%. Representative feldspar analyses from each sample are listed in Table 1. Table 1 also gives the average detection limits and precision of these feldspar analyses (Nicholls and Stout, 1986).

Prior to analysis, each thin section had been etched with acid for Nomarski imaging. Consequently, each sample was repolished enough to remove any topography (Clark et al., 1986) and to ensure that the plagioclase analyzed was not affected by the etching. Analytical points were located precisely with the use of plane-polarized light photomicrographs of each sample. The locations of analyses were plotted on each photomicrograph with reference to optically discernible resorption surfaces, mineral or glass inclusions, or the edges of crystals. The reproducibility of the spot locations is no better than two beam diameters.

Laser interferometry

A complete description of this technique may be found in Pearce (1984b). To summarize, polarized coherent green light (wavelength = 514.5 nm) is produced from a Spectra-Physics 164 Ar-ion laser operating at a few hundred milliwatts. The source laser beam passes through a spatial filter and collimator that expands the beam and produces a planar wave front. A beam splitter separates the light into a reference beam that bypasses the thin section and a sample beam that travels through a plagioclase crystal in the polished thin section. The wave front of the sample beam becomes encoded with information about the magnitude and distribution of refractive index in the crystal. The sample beam is then allowed to interfere with the reference beam at a second beam splitter. The resultant linear narrow fringes are shifted from zone to zone in the interferogram ("image") of the crystal because of changes in refractive index (a result of changes in plagioclase composition from zone to zone).

The fringes (Figs. 1C, 1G, 2C, 2G, 3B, 3D, 3F, 3H) may be interpreted as graphs of refractive index and hence composition. (The photographs in each figure are usually arranged in such a way that those with increasing An content are toward the top.) The scale is such that a fringe shift of one apparent wavelength is 33 An% as indicated in Figure 3. Careful measurement and digitizing of these fringes establishes the relative plagioclase compositions

→

Fig. 2. Examples of banded type II and large sieve-textured type I plagioclase. (A) Photomicrograph (cross-polarized light) of crystal MSH-D-1. Note the distinctive banded appearance of the crystal. (B) Nomarski image of the etched polished surface of the above crystal. Over 20 zones are revealed by etching. The banded nature of this crystal is further brought out by this technique. Relatively sodic bands, e.g., the rim, appear as topographic highs whereas more calcic bands (CP) appear as troughs or topographic lows. "R" indicates resorption surface. Zonal widths range from 2.5 to 35 μm in this crystal with an average of about 7.5 μm. (C) Narrow-fringe laser interferogram (514.5 nm) of the above crystal. The banded nature of this crystal is also observed in this symmetrical view of the fringes. Note that the calcic highs appear as "plateaus" (CP) in the fringe pattern. (D) Digitized profiles of the interferogram in Fig. 2C extending from the core (C) to the rim (X). Note that the banded nature of the zoning is even more obvious in this representation. Each zone appears to have even-oscillatory zoning, but there are distinct breaks in composition between the major zones. (E) Photomicrograph (cross-polarized light) of large (type I) crystal MSH-A-5. Note the severely resorbed core. The outermost, finely banded mantle of the crystal is about 100 μm wide. (F) Nomarski image of etched crystal MSH-A-5. The finely zoned mantle deposited upon the core is evident in this image. The fine bands in the outermost mantle of the crystal average about 10 μm in thickness and are for the most part euhedral. Note the crosscutting relationship of the fracture in the lower right-hand corner of the crystal and the missing fragment directly below it. This fracturing event took place immediately prior to vesiculation as the fine vesicle walls are unfractured. (G) Narrow-fringe laser interferogram (514.5 nm) of the crystal in Fig. 2F. Note the essentially flat or even nature of the zoning. There is a double rim to the crystal located in the region of the surfaces marked "R" and "X." "R" indicates a resorption surface; "X" is the outermost rim. (H) Digitized profile of the interferogram in Fig. 2G (traverse X to C). Note the double normally zoned rim on the essentially flat zoning profile. Note that the zoning profile may be traced right through the strongly resorbed core as a "ghost" fringe in Fig. 2G.

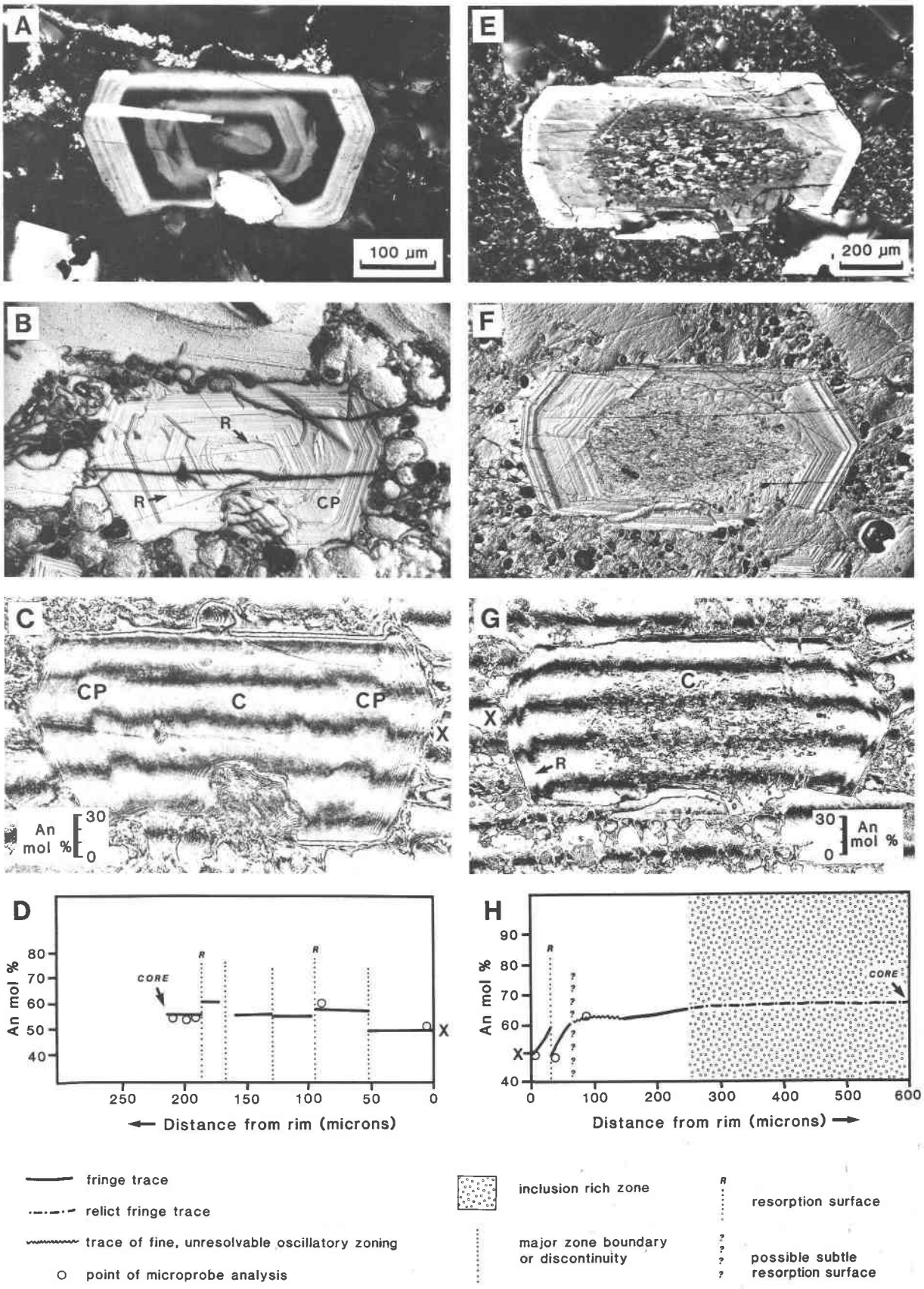
A
100 μm
E
200 μm
B
R
R
CP
F
C
CP
C
CP
X
An mol %
30
0
G
C
X
R
30
0
An mol %
D
An mol %
80
70
60
50
40
CORE
R
R
X
250
200
150
100
50
0
← Distance from rim (microns)
H
An mol %
90
80
70
60
X
40
R
CORE
0
100
200
300
400
500
600
Distance from rim (microns) →
fringe trace
relict fringe trace
trace of fine, unresolvable oscillatory zoning
point of microprobe analysis
inclusion rich zone
major zone boundary or discontinuity
R
resorption surface
possible subtle resorption surface

between zones. Electron-microprobe analyses of selected sites on each crystal serve to determine absolute An contents, which in turn lead to absolute An determinations for each zone.

Nomarski contrast interferometry

The Nomarski interference-contrast technique serves to enhance zonal and discontinouous features of etched plagioclase phenocrysts (see Anderson, 1983, 1984, and Clark et al., 1986, for further details). Plagioclase is etched with fluoboric acid HBF_4, which is then neutralized by immersion in a saturated solution of Na_2CO_3. Zones containing relatively more Ca are etched more deeply than those zones containing less Ca, thus producing a microtopographic relief of highs (sodic) and lows (calcic). The polished thin sections are rinsed with water and dried; a C coat is added to the surface to increase reflectivity and eliminate internal reflections within the phenocrysts. Although revealing very fine textural details of zonation, this technique does not readily indicate composition.

Observations

The dull grayish-white pumice that we have studied is typical of the May 18 pyroclastic flows. The petrography of our sample agrees with that of Kuntz et al. (1981), and the reader is referred to that paper for a more detailed petrographic analysis of the pumice. Generally, the pumice sample is a fine-grained mixture of plagioclase, hornblende, hypersthene, and trace opaques (magnetite) within a highly vesiculated glass. Our modal analyses (not counting the vesicles) are glass 64.6% (62.1), plagioclase 26.1% (30.0), orthopyroxene 3.0% (4.2), hornblende 3.9% (2.5), and opaques 2.2% (1.2) and agree with those of Kuntz et al. (1981), shown in parentheses. The volume of vesicles in our sample was found to be 69.7% compared with 71% reported by the latter authors. This is remarkable agreement considering that we determined the glass/vesicle ratio by point counting an etched polished section in reflected light using Nomarski interference contrast, whereas Kuntz et al. determined this ratio from bulk-density data. As in the work of Kuntz et al., we found clinopyroxene to be quite rare (one crystal in six thin sections). All nonopaques contain variable amounts of a pale green, nonpleochroic, acicular mineral (average size: 5 × 30 μm) that may be apatite.

Hornblende occurs as subhedral to anhedral cross sections and elongate laths about 100 to 300 μm in length. About half the observed crystals exhibit features that we prefer to interpret as being due to resorption, although an alternative explanation might be conditions of growth leading to rounded growth forms. Irregular rounded edges, re-entrants, and minor sieve textures (which may be cross sections of re-entrants) are all common in hornblende crystals. This contrasts with the findings of Cashman and Taggart (1983) and Scarfe et al. (1982) who studied products of later eruptions. As we find no evidence of reaction coronas, the hornblende appears to have simply dissolved with no reaction products being formed. Hornblende has intergrown with plagioclase, includes plagioclase, or is included in plagioclase. In some instances, amphibole appears to have initiated convolute zoning in the plagioclase host. Hypersthene commonly occurs as 150- to 200-μm equant grains; resorbed or spongy phenocrysts are rare, although we show one example of strongly resorbed (spongy) hypersthene (Fig. 4E).

Plagioclase occurs mainly as individual subhedral to euhedral laths up to 2.7 mm long. The pumice contains minor amounts of mutually intergrown plagioclase crystals and rare intergrowths of plagioclase with hornblende, hypersthene, and opaques. Plagioclase contains inclusions of glass, acicular apatite (commonly restricted to specific zones), hornblende, magnetite and, rarely, hypersthene. Twinning is not very common but where present occurs according to the albite, Carlsbad-albite, and pericline twin laws.

Plagioclase compositions vary from An_{37} to An_{63}. Plagioclase microphenocrysts appear to occur in two size populations that we refer to as type I (larger) and type II (smaller euhedral). Most of the plagioclase crystals are of the smaller size group (type II), ranging from 50 to 700 μm (rarely up to 1200 μm) in length. They are typically even-oscillatory to normal-oscillatory zoned, with fine

→

Fig. 3. Photomicrographs and laser interferograms of Mount St. Helens plagioclase crystals. (A) Photomicrograph (cross-polarized light) of crystal MSH-A-2. (B) Narrow-fringe laser interferogram (514.5 nm) of crystal MSH-A-2 (Fig. 3A). Note the even-oscillatory-zoned nature of this crystal. The core (C) is An_{52}, and the mantle is An_{42}. Zone widths (in reflected-light Nomarski) are from 2.5 to 7.5 μm and average 3.0 μm. There is no discernible rim. (C) Photomicrograph (cross-polarized light) of a slightly banded, even-oscillatory-zoned crystal (MSH-A-1). "ST" indicates a sodic trough, and "R" indicates a resorption surface. (D) Narrow-fringe laser interferogram (514.5 nm) of crystal MSH-A-1 (Fig. 3C). A small core region is indicated by "C." "ST" indicates the sodic trough, and "R" indicates a resorption event that followed the deposition of the sodic trough. Note the even nature of the oscillatory zoning on the outside of the surface indicated by "R." There is no discernible rim. (E) Photomicrograph (cross-polarized light) of crystal MSH-D-11. Note that the birefringence in this crystal indicates a greater fluctuation in An content than is common for crystals of this size. (F) Narrow-fringe laser interferogram (514.5 nm) of crystal MSH-D-11 (Fig. 3E). Note the resorption surfaces (R) usually followed by an increase in Ca content shown by the calcic spikes. This increase may be as much as 15 mol%. The core composition is 44 mol% An; the average composition after resorption is 50 mol% An. There appears to be a slight, normally zoned rim. (G) Photomicrograph (cross-polarized light) of crystal MSH-A-3. Note the banded nature of the zoning and the slightly more extreme birefringence compared with crystal MSH-A-1, for example, in Fig. 3C. (H) Narrow-fringe laser interferogram (514.5 nm) of crystal MSH-A-3 (Fig. 3G). Note the general resemblance of this pattern to that of Fig. 3F. Resorption events indicated by "R" are followed by a sharp increase in An content (calcic "spikes"). The core composition for this crystal is An_{52}, the rim is about An_{50}, and zone widths (reflected-light Nomarski) vary from 2.5 to 14 μm and average 2.9 μm.

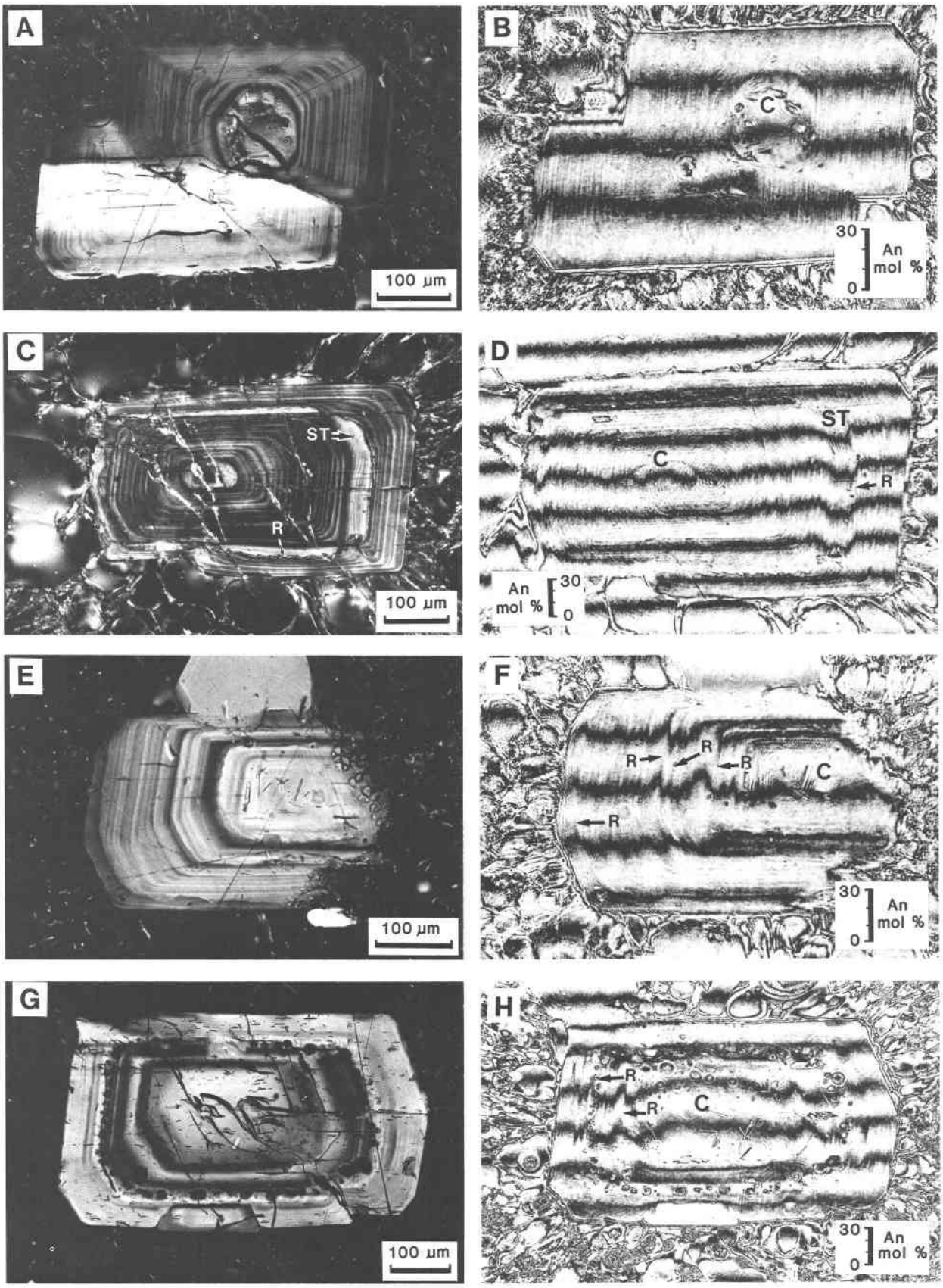
A
100 μm
B
C
30
An
mol %
0
C
ST
R
100 μm
D
ST
C
R
An
mol %
30
0
E
100 μm
F
R
R
R
C
R
30
An
mol %
0
G
100 μm
H
R
R
C
30
An
mol %
0

oscillations ranging in width from 2 to 50 μm, but typically averaging 10 μm. Reverse zoning is rare.

Most of the larger (type I) plagioclase crystals (the xenocrysts or the earliest generation of plagioclase, as suggested by Kuntz et al., 1981) have broad homogeneous cores of An_{60-63} (up to 700 μm wide). These are surrounded by a mantle of An_{45-50} (200 to 300 μm thick), containing even- to normal-oscillatory zoning. The core is commonly characterized by many glass inclusions and patchy extinction (e.g., Figs. 2E, 4C). The glass inclusions are square to vermicular in shape. Larger inclusions (up to 200 μm long) occur within the center of the core and are usually interconnected to form a sinuous network. They decrease in size toward the outer areas of the core, becoming individual rounded inclusions (with similar appearance to the "dusty inclusions" of Tsuchiyama, 1985). These type I phenocrysts are almost invariably broken or breached in some manner. On textural grounds, this period of fracturing appears to be the last event affecting the phenocrysts, and we tentatively identify this as the catastrophic eruption of May 18, 1980. The outer finely banded zones do not generally appear to have been affected by resorption although there are exceptions (e.g., MSH-D-8 in Fig. 4C). A few of the phenocrysts have albite twinning, and one large (2.7 mm) crystal was observed.

Most plagioclase crystals have at least one notable discontinuity that cuts across earlier zones and may therefore be identified as a resorption surface. Because of the repetition of this feature stratigraphically within a single phenocryst (see Figs. 1B, 1C, and 1D), we do not consider that these discontinuities can be due to growth of hollow cores, later filled in with plagioclase of a different composition. These resorption surfaces have a variety of morphologies, some of which appear remarkably similar to sedimentary depositional and erosional structures. Embayments cutting earlier zones are usually less than 10 μm in depth (see Fig. 4B) and may have associated glass, opaques, and/or acicular inclusions trapped by post-solution crystallization. The development of simple to complex convolute zoning appears locally associated with inclusions. Most of the crystals show an increase in An content after these discontinuities, which may equal or exceed the An content of the core area.

Electron-microprobe analysis

Plagioclase crystals from three polished thin sections (MSH-A, MSH-B, MSH-D) were analyzed by electron microprobe. The electron-microprobe data provide an independent means of evaluating the compositional differences within and between plagioclase grains. The analyses also provide a reference composition to quantify the interferograms. Representative feldspar analyses are reported in Table 1 for the plagioclase crystals discussed in the text. The reported analyses represent the most and least An-rich zones that were analyzed in each crystal.

TABLE 2. Representative electron-microprobe analysis of orthopyroxene from the Mount St. Helens pumice

Oxide	Wt%	Cations	
SiO_2	52.84	Si	1.9569
Al_2O_3	0.97	Al	0.0423
FeO	21.42	Fe	0.6634
MgO	23.87	Mg	1.3176
CaO	1.05	Ca	0.0417
Total	100.15		4.0219

Note: Values are averages for five spots on a single grain from thin section MSH-A.

In characterizing the compositional ranges of the individual plagioclase crystals, we attempted to analyze, where possible, (1) compositionally homogeneous cores of crystals, (2) extreme edges of crystals, and (3) at least one side of any major resorption surface. Analyses that belong to category 3 were difficult to reproduce because of the topographic complexity of the resorption surfaces. In several instances, such surfaces were associated with strong oscillatory zoning (see Fig. 1D or 2H). These resorption surfaces may also be repeated over a very narrow width. Consequently, the measurement of these composition shifts by electron microprobe can be imprecise. In such instances, the microprobe analysis may represent an average composition. Figures 1D, 1H, 2D, and 2H illustrate a very good match between the compositional shifts measured by electron-microprobe analysis and laser interferometry.

To confirm that the material we have used is similar to that worked on by the experimental petrologists, we have analyzed some of the mineral phases. Our results compare favorably with those of Rutherford et al. (1985, Table 6) and Scheidegger et al. (1982, Tables 2 and 3). The composition of a single pyroxene crystal from section MSH-A is listed in Table 2. The analysis is an average of five points on a single orthopyroxene crystal. Table 3 presents partial electron-microprobe analyses for the matrix glass of the MSH pumice. The averages of analyses for the three polished thin sections agree to well within the analytical precision of the instrument. The matrix glass is homogeneous in composition, at least on a thin-section scale, and is inferred to represent the melt composition that last equilibrated with the phenocrysts prior to eruption.

→

Fig. 4. Resorption and discontinuous features in plagioclase and other minerals in the pumice. "R" denotes a resorption or solution surface. (A) Nomarski image of a banded plagioclase crystal (MSH-D-1) showing a rounded, anhedral center and wavy zones throughout. Subsequent layers of plagioclase infill the irregularities to achieve the straight edges of a euhedral crystal form. (B) Nomarski image showing an apparent solution surface cutting through layers in plagioclase crystal MSH-D-9. The embayment

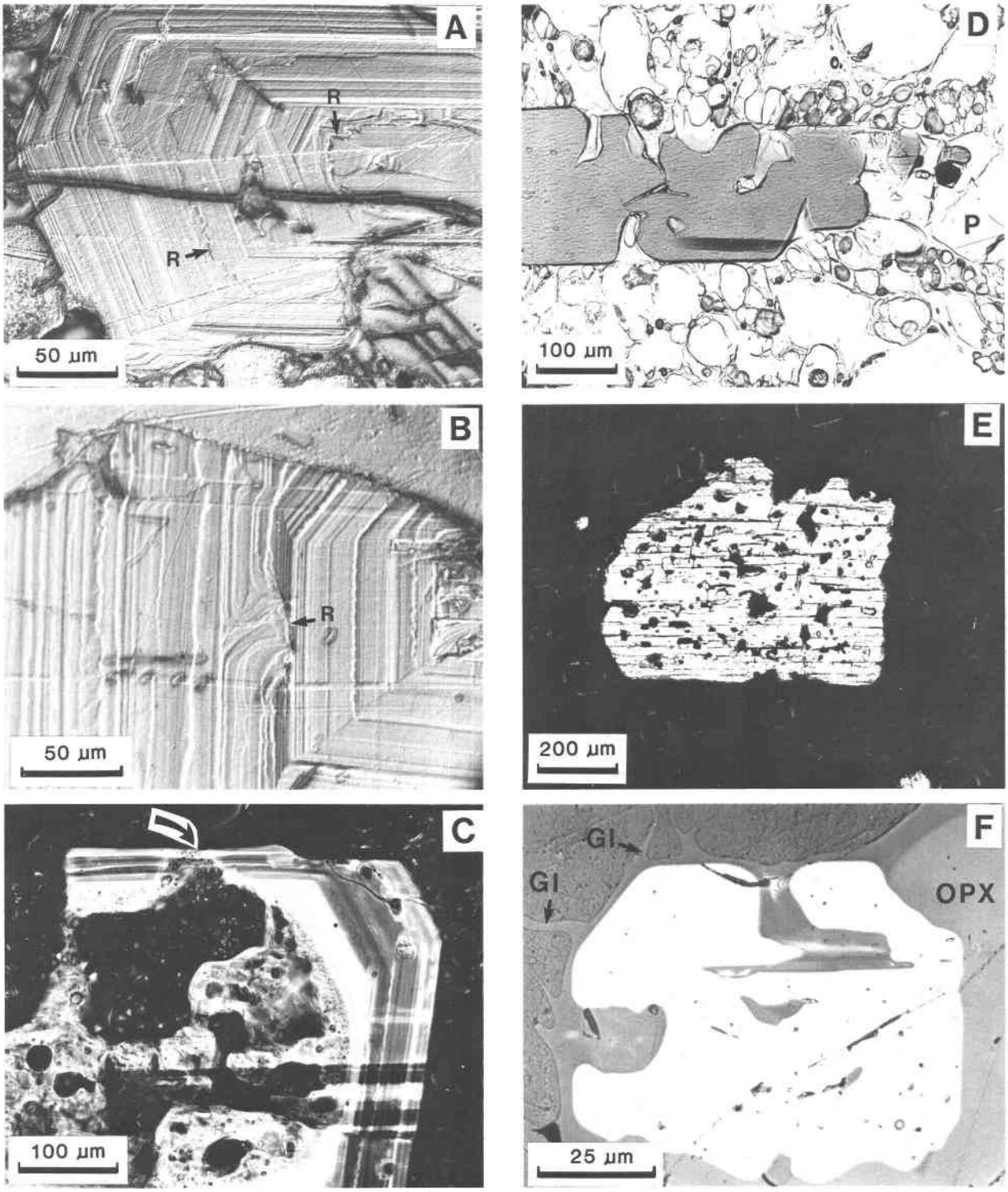

at "R" is infilled by convolute zones around an unseen glass inclusion (observed in transmitted light). (C) Photomicrograph (cross-polarized light) of a large sieve-textured plagioclase (MSH-D-8) with central alteration that appears to have spread outward toward the rim. Note the breach (shown by an arrow) that appears to crosscut the straight zones in the crystal rim. (D) Photomicrograph (cross-polarized light) of an irregularly shaped and broken hornblende—a common occurrence in this pumice sample. Part of this hornblende is included in a plagioclase crystal (P). (E) Photomicrograph (cross-polarized light) of sieve-textured hypersthene—an uncommon occurrence in this pumice sample. (F) Reflected-light photomicrograph of an anhedral, rounded magnetite crystal, partially enclosed within a hypersthene crystal (OPX). The narrow glass vesicle walls are denoted by Gl.

TABLE 3. Representative whole-rock chemical analyses of the Mount St. Helens pumice

	Whole rock		Partial glass analyses		
	MSH-1	MSH-2	A(n = 14)	B(n = 11)	D(n = 13)
SiO_2	64.83	65.31	71.98	71.90	72.15
TiO_2	0.63	0.62	n.d.	n.d.	n.d.
Al_2O_3	18.17	18.15	15.17	15.09	15.08
FeO	3.94	3.92	2.30	2.27	2.30
MnO	0.07	0.07	0.07	0.06	0.07
MgO	1.55	1.57	0.61	0.59	0.56
CaO	4.87	4.87	2.46	2.48	2.44
Na_2O	5.01	4.95	3.37	3.21	3.27
K_2O	1.36	1.36	2.02	2.03	2.05
P_2O_5	0.17	0.17	n.d.	n.d.	n.d.
Total	100.60	100.99	97.98	97.63	97.92

Note: Materials for whole-rock analysis are from samples MSH-1, -2. Analysis is by X-ray fluorescence using fused discs with a lithium-metaborite flux. Also reported are partial electron-microprobe analyses of the glass matrix for samples MSH-A, -B, -D. The values reported are the average of 10 or more (n) electron-microprobe analyses.

Laser interferometry observations

Cores of the type I crystals tend to be An_{60-63}, whereas their finely oscillatory-zoned mantles are An_{45-55} (Figs. 2E to 3H). Interferograms show that the cores tend to be fairly uniform in composition with generally no more than 5% An differences. Narrow rims of different compositions are not well developed in either type I or type II crystals, although there is a tendency for slightly more calcic plagioclase (An_{48-59}) at the outer edges of some crystals. Most crystals (see Figs. 1C, 2C, 3B, and 3D) have no discernible rim in contrast to those from dacitic lavas from Mount St. Helens (not shown) which commonly have discrete rims of significantly different composition (Pearce, unpub. data). In the case of the type II crystals, the overall background composition is typically An_{47}, on which abrupt changes in composition may be superimposed. Sodic "troughs" in the profiles, of compositions as low as An_{37}, are locally present (see Fig. 3D, for example). More rare are calcic "plateaus" in the profile that may, in some cases, be up to An_{60}, such as that of Fig. 2C. Locally, there are more complicated fluctuations in composition of up to 20 mol% An across the discontinuity (see Figs. 1C, 1D, 3F, and 3H). In contrast to the general patterns just described, some crystals have a completely flat, even-oscillatory pattern with very small oscillations in An (about 1 to 3%). In the case of crystal MSH-A-2 (Figs. 3A, 3B), optical determinations indicate that the crystal has a "flat" mantle (An_{42}) surrounding a core of An_{52}.

We consider, along with other workers (for example, Bottinga et al., 1966, and Sibley et al., 1976; see also Smith, 1974), that the small-scale fluctuations are due to extremely local, diffusion-controlled interactions of the crystal with the boundary layer surrounding it. If we attribute the larger abrupt changes in composition to large-scale changes in magmatic conditions (P_{H_2O}, temperature, etc.; see Smith and Lofgren, 1983), then we must conclude that individual crystals appear to have unique histories that, although similar in overall aspect, are different in detail. If we assume that magmatic conditions (P, T, etc.) affect the composition of the growing crystals, then it seems impossible for all the crystals in Figure 3, for example, to have grown under exactly the same set of magmatic conditions. Similarly, the sodic trough of MSH-A-1 (Fig. 3D) is incompatible with the calcic plateau of MSH-D-1 (Fig. 2C). Note that these two crystals are the same size and the abrupt change in composition occurs at about the same stage of growth in both crystals. This appears to imply that magmatic conditions were not uniform even on the scale of a microphenocryst or, perhaps more likely, our dacitic material contains more than one population of crystals. Either prior to or during the eruption, there was mixing of dacitic material with a variable crystallization history. We are not aware of any study on the homogeneity of the glass that might indicate mixing of different liquids.

Nomarski contrast-interferometry observations

Nomarski imaging of etched polished surfaces reveals detailed zoning and other textural features not readily seen in transmitted light. For example, the details of the glass vesicle walls in the pumice are clearly revealed in Figure 4F. The volume ratio of glass/vesicle space is also readily determined from observations of this type. Convolute zoning (associated with an inclusion and resorption surface) is shown in Figure 4B (at the point marked "R"). We have found this inclusion and convolute zoning association in other rocks, and we consider that it is of general occurrence.

Nomarski imaging of zoning is especially valuable in identifying cross cutting features associated with solution surfaces in otherwise euhedral zonation. An example is plagioclase MSH-B-1 in Fig. 1F, a microphenocryst containing remarkably euhedral zones with the exception of several resorption surfaces marked "R." Similar features are evident in the crystal of Figure 1B, which, however, has more resorption surfaces. The euhedral form that is so important in determining the origin of some types of oscillatory zoning is sometimes indistinct in transmitted light but is quite clearly defined in Nomarski observations. Examples of the exact resolution of euhedral zone shape are shown in Figures 1B, 1F, 2B, 2F, 4A, and 4B. A radius of curvature at the corner of a zone as small as 1 μm may be detected in this manner. Such detail is beyond normal resolution in transmitted light using a slide with a thickness of 30 μm. The euhedral nature of this type of zoning, we consider, is compatible with abrupt cessation of growth followed by renewed growth, commonly of a more calcic plagioclase without any trace of a solution event between the zones. This type of zonation implies a diffusion-controlled, local-boundary-layer mechanism as suggested by numerous authors among whom are Bottinga et al. (1966), Sibley et al. (1976), and Pearce (1984c).

Nomarski imaging tends to reveal more zones and narrower zones than conventional microscopy. For example, banded plagioclase MSH-D-9 appears to contain 39 os-

cillatory zones in transmitted light (Fig. 1A; crossed Nicols). In reflected light (Fig. 1B), the same crystal shows at least 58 zones. The average thickness of 550 zones measured in 24 crystals is 6.6 μm (standard deviation, 7.6) in transmitted light and 4.2 μm (standard deviation, 1.5) in reflected light. Clearly, Nomarski observation in reflected light reveals much more detail than conventional transmitted-light microscopy, and we recommend its use in studies in which the detailed observation of oscillatory zoning is important.

Discussion

Our observations indicate that the dacite magma that formed the pumice fragment we have studied in this work contained at least two populations of phenocrysts. These populations are characterized in part by both the presence or absence, and the type, of resorption features. These two populations may represent samples of a zoned magma chamber (see Melson and Hopson, 1982) or the mixing of different magmatic phases during eruption. There is an overlap in the patterns of zoning composition between the large (type I, typically more than 1-mm diameter) plagioclase crystals with spongy cores, referred to as "xenocrysts" by Kuntz et al. (1981), and the small (type II, typically less than 700-μm diameter) euhedral crystals that generally lack massive resorption features. The outer, finely zoned mantles (200 to 300 μm thick) of the large crystals appear to correspond to the complete growth pattern of smaller crystals (one-half diameter = 200 to 300 μm). The compositions of both are approximately the same (An_{55-45}); and the zoning profiles from laser interferograms appear, at least superficially, to be similar in their general features. For this period of crystallization, there were no strong resorption events and no great changes (more than 20 mol% An) in composition. Because of this apparent overlap, we regard most of the large crystals as either early-formed phenocrysts or comagmatic xenocrysts. We prefer the former explanation.

Considering the work of Cashman and Marsh (1984), and using the crystal-size distribution theory of Marsh (1984), we speculate that the mantles of the large phenocrysts (because of their similar thicknesses) correspond in time to the complete growth history of the smaller phenocrysts. Most of the type II microphenocrysts appear to postdate the massive resorption event indicated by the spongy interiors of the large crystals although there may have been some overlap. We estimate the time for growth of the type II crystals to be about 2000 d at a growth rate of 0.1 μm/d. We emphasize that this is only an order-of-magnitude estimate.

There is no evidence of plagioclase overgrowth or of solution enlargement postdating the fractures in the type I crystals. The fracturing event that commonly shattered these phenocrysts appears to be the last event that affected them. We correlate this event with the disruption of the magma by magma fracturing during the Plinian eruption of May 18, 1980. We consider it possible that the relatively large volume of magma within the spongy interiors of the crystals may have expanded with sufficient force during magma fracturing to physically shatter the large phenocrysts. This explanation requires substantiation; however, it is consistent with petrographic observations that some fragments, embedded in pumiceous matrix, may be fitted together to form an unfractured crystal (Fig. 2F).

In keeping with our assumption that rounded forms are most likely due to solution, and our observation that there is an overlap of composition between the type I and type II plagioclase phenocrysts, our detailed model based on our observations, as well as those of previous workers, is as follows:

1. Crystallization at depth (possibly greater than 7 km). Plagioclase, possibly accompanied by amphibole, orthopyroxene, magnetite, and apatite, was stable at this stage of crystallization. The plagioclase composition was approximately An_{60}, and the crystals grew to a diameter of 600 to 700 μm. If the work of Cashman and Marsh (1984) is applicable for this stage of growth of the plagioclase, this event might have taken about 2000 d.

2. A massive resorption event, probably due to upward transport and pressure release. All of the phases were unstable during this event and began to dissolve in the magma. At this point, the plagioclase developed the spongy appearance first recorded by Kuntz et al. (1981). It is possible that during this event, if it was indeed due to upward transport, there was a mixing of different layers of the magma since some of the phenocrysts do not appear to have been severely resorbed. Hornblende was resorbed and did not react with the magma.

3. Crystallization at lower pressure with only plagioclase being the stable phase. The plagioclase has a composition of An_{55-45}, but typically An_{47}. It is possible that orthopyroxene was also stable at this stage; however, we have not enough evidence to decide this unequivocally. This phase of development of the magma might correspond to the cupola of Sigurdsson et al. (1984) or the upper part of the zoned chamber of Melson and Hopson (1982). From our work, we cannot determine the depth of the magma at stage 3. At this point in the development of the magma, additional centers of plagioclase growth occurred, and type II (200- to 700-μm diameter) crystals grew contemporaneously with the overgrowths of the preexisting, partially resorbed type I plagioclase. This resulted in large (type I) crystals with finely zoned exteriors and spongy interiors. During this period of growth, abrupt changes in the stable composition of plagioclase occurred. These changes yielded a characteristic banded aspect to the zoning in laser interferograms. It is notable that sodic troughs are present in some crystals whereas calcic "plateaus" occur in others. It is not known at this time what caused these slight yet distinct changes in compositional zoning profiles. Further work needs to be done on this aspect of the Mount St. Helens problem. Nomarski imaging and transmitted-light microscopy clearly indicate that periods of resorption of the plagioclase occurred during this growth stage.

4. The eruption of May 18 accompanied by magma fracturing (Sigurdsson et al., 1984) and disruption of the type I plagioclase. It is notable that there are no quench crystals or skeletal overgrowths on any of the phases or in the glass, such was the rapidity of the eruption and subsequent quenching of the liquid.

We emphasize that the above model is the simplest model that could explain the petrographic details we have observed. We recognize that there are some microphenocrysts present in minor amounts that do not fit our simple two-stage model, and we regard these as probably being cognate xenocrysts. The complex pattern of resorption events present in some crystals (e.g., Fig. 1D) indicates that a two-stage model is, at best, a first approximation. However, we believe such a model is an essential step in the understanding of the complexities of the actual volcanic events. It is interesting that Cashman and Marsh (1984), working on later dacite flows of the period 1980–1982, identified two cooling events—one at depth and another after upward transport. In our model, however, we consider that the two major stages of growth took place "at depth" prior to eruption.

Conclusions

The sample we have examined appears to contain more than one population of phenocrysts and may itself be an example of different layers in a zoned magma chamber. A common sequence of events can be determined for most of the phenocrysts in the sample and involves an early stage of massive resorption of all phenocryst stages. The resorption of hornblende with no sign of magmatic reaction or opacite rims is remarkable. We consider that this is very unusual for this rock type. There is a general similarity in zoning patterns between the mantles of the larger phenocrysts and the complete zoning patterns of smaller euhedral phenocrysts of plagioclase. We consider that this is due to contemporaneous growth. In spite of evident similarities in zoning profiles of different crystals, we are reluctant to draw an exact correlation between specific events, pending more detailed magmatic stratigraphic correlation work between phenocrysts. A study of magmatic crystal stratigraphy and inferred magmatic conditions is now in progress and will be reported at a later date.

Acknowledgments

The research in this study was supported by Natural Sciences and Engineering Research Council of Canada Operating Grant A88709 and Infrastructure Grant A0656 (T.H.P.). The photographic Nomarski microscope system was funded by an NSERC grant to T.H.P. and A. H. Clark. Acknowledgment is made by J.K.R. for funding through NSERC Grant 67-5112 (UBC research services). Electron-microprobe analyses were obtained at the University of Calgary SEMQ-ARL installation. This research is partly a result of theoretical work done in connection with studies of zoned crystals using a new laser interference microscope (Canadian Patent Number 1,163,797, U.S. patent pending, application no. 558,590). The laser-equipped microscope laboratory at Queen's University was funded by an NSERC New Research Idea Grant A5226 and NSERC Equipment Grants E6622, E1449, E5784, and E0296.

Carol Luce did the drafting and modal analyses, Dawn Crawford typed data files, and Craig Rice obtained statistical data on frequency and widths of zonation. This manuscript benefitted from review by M. J. Rutherford. Part of the initial research in this study was supported by grants from the Graduate School and the Advisory Research Committee, Queen's University.

References cited

Anderson, A.T., Jr. (1983) Oscillatory zoning of plagioclase: Nomarski interference contrast microscopy of etched sections. American Mineralogist, 68, 125–129.

——— (1984) Probable relations between plagioclase zoning and magma dynamics, Fuego volcano, Guatemala. American Mineralogist, 69, 660–676.

Bence, A.E., and Albee, A.L. (1968) Empirical correction factors for the electron microanalysis of silicates and oxides. Journal of Geology, 76, 382–403.

Bottinga, Y., Kudo, A., and Weill, D. (1966) Some observations on oscillatory zoning and crystallization of magmatic plagioclase. American Mineralogist, 51, 792–806.

Cashman, K.V., and Marsh, B.D. (1984) Crystal-size spectra and kinetics of crystal growth in magma: II. Application. Geological Society of America Abstracts with Programs, 16, 465.

Cashman, K.V., and Taggart, J.E. (1983) Petrologic monitoring 1981 and 1982 eruptive products from Mount St. Helens. Science, 221, 1385–1387.

Clark, A.H., Pearce, T.H., Roeder, P.L., and Wolfson, I. (1986) Oscillatory zoning and other microstructures in magmatic olivine and augite: Nomarski interference contrast observations on etched polished surfaces. American Mineralogist, 7, 734–741.

Kuntz, M.A., Rowley, P.D., MacLeod, N.S., Reynolds, R.L., McBroome, L.A., Kaplan, A.M., and Lidke, D.J. (1981) Petrography and particle-size distribution of pyroclastic-flow, ash-cloud, and surge deposits. In P.W. Lipman and D.R. Mullineaux, Eds., The 1980 eruptions of Mount St. Helens, Washington. U.S. Geological Survey Professional Paper 1250, 525–539.

Leeman, W.P., and Smith, D.R. (1982) Petrology of Quaternary volcanic rocks from Mount St. Helens and vicinity. EOS, 63, 1144.

Lipman, P.W., and Mullineaux, D.R., Eds. (1981) The 1980 eruptions of Mount St. Helens, Washington. U.S. Geological Survey Professional Paper 1250, 844 p.

Marsh, B.D. (1984) Crystal-size spectra and kinetics of crystal growth in magma: I. Theory. Geological Society of America Abstracts with Programs, 16, 585.

Melson, W.G. (1983) Monitoring the 1980–1982 eruptions of Mount St. Helens: Compositions and abundances of glass. Science, 221, 1387–1391.

Melson, W.G., and Hopson, C.A. (1982) Petrologic model of the 1980–82 Mount St. Helens magma chamber. EOS, 63, 1144.

Merzbacher, C.I., and Eggler, D.H. (1984) A magmatic geohygrometer: Applications to Mount St. Helens and other dacitic magmas. Geology, 12, 587–590.

Nicholls, J., and Stout, M.Z. (1986) Electron beam analytical instruments and the determination of modes, spatial variations of minerals and textural features of rocks in polished thin sections. Contributions to Mineralogy and Petrology, 94, 395–404.

Nicholls, J., Fiesinger, D.W., and Ethier, V.G. (1977) Fortran IV programs for processing routine electron microprobe data. Computers & Geoscience, 3, 49–83.

Pearce, T.H. (1984a) The analysis of zoning in magmatic crystals with emphasis on olivine. Contributions to Mineralogy and Petrology, 86, 149–154.

——— (1984b) Multiple frequency laser interference microscopy: A new technique. The Microscope, 32, 69–81.

——— (1984c) Optical dispersion and zoning in magmatic plagioclase: Laser interference observations. Canadian Mineralogist, 22, 383–390.

Rowley, P.D., Kuntz, M.A., and MacLeod, N.S. (1981) Pyroclastic-flow deposits. In P.W. Lipman and D.R. Mullineaux, Eds., The 1980 eruptions of Mount St. Helens, Washington. U.S. Geological Survey Professional Paper 1250, 489–512.

Rutherford, M.J., and Devine, J. (1986) Experimental petrology of recent

Mount St. Helens dacites: Amphibole, Fe-Ti oxides and magma chamber conditions. Geological Society of America Abstracts with Programs, 18, 736.

Rutherford, M.J., Sigurdsson, H., Carey, S., and Davis, A. (1985) The May 18, 1980, eruption of Mount St. Helens: 1. Melt composition and experimental phase equilibria. Journal of Geophysical Research, 90, 2929–2947.

Scarfe, C.M., Fujii, T., and Harris, D.M. (1982) Mineralogy and geochemistry of pumice from 19 March 1982 eruption of Mount St. Helens. Geological Society of American Abstracts with Programs, 14, 608.

Scheidegger, K.F., Federman, A.N., and Tallman, A.M. (1982) Compositional heterogeneity of tephras from the 1980 eruptions of Mount St. Helens. Journal of Geophysical Research, 87, 10,861–10,881.

Sibley, D.F., Vogel, T.A., Walker, B.M., and Byerly, G. (1976) The origin of oscillatory zoning in plagioclase: A diffusion and growth controlled model. American Journal of Science, 276, 275–284.

Sigurdsson, H., Rutherford, M., and Carey, S. (1984) Conditions in the Mount St. Helens magmatic reservoir and dynamics of the 18 May 1980 Plinian eruption: Experimental petrology and physical modelling. In M.A. Dungan, T.L. Grove, and W. Hildreth, Eds., Proceedings of the open magmatic systems, p. 141–143. Southern Methodist University, Dallas, Texas.

Smith, J.V. (1974) Feldspar minerals: 2. Chemical and textural properties. Springer-Verlag, New York, 690 p.

Smith, R.K., and Lofgren, G.E. (1983) An analytical and experimental study of zoning in plagioclase. Lithos, 16, 153–168.

Tsuchiyama, A. (1985) Dissolution kinetics of plagioclase in the melt of the system diopside-albite-anorthite, and origin of dusty plagioclase in andesites. Contributions to Mineralogy and Petrology, 89, 1–16.

Manuscript received December 23, 1986
Manuscript accepted June 26, 1987